Available online at https://asric.africa/engineering-sciences
ASRIC Journal of Engineering Sciences Vol.5(2)(2025) 68-91

Remote Sensing of Chlorophyll-A Concentrations in a Water Hyacinth-Infested Tropical Headwaters Lake: A Study of Lake Tana, Ethiopia

Bekalu W. Asres[a], Mebrahtom G. Kebedew[b], Meareg D. Nerae[c], Seneshaw Tsegaye[b*], Fasikaw A. Zimale[d]

[a] School of Civil and Water Resource Engineering, Debre Markos Institute of Technology, Debre Markos University, Debre Markos, Ethiopia: beki.manalie19@gmail.com (B.W.A.)

[b] Department of Bioengineering, Civil Engineering and Environmental Engineering, U.A. Whitaker College of Engineering, Florida Gulf Coast University, 10501 FGCU Blvd. So., Fort Myers, FL 33965, USA: mkebedew@fgcu.edu (M.G.K.); stsegaye@fgcu.edu (S.T.)

[c] School of Civil Engineering, Ethiopian Institute of Technology- Mekelle, Mekelle University, Mekelle, Ethiopia: mearegdesta1@gmail.com (M.D.N.)

[d] Faculty of Civil and Water Resources Engineering, Bahir Dar Institute of Technology, Bahir Dar University, Bahir Dar, Ethiopia: fasikaw@gmail.com (F.A.Z.)

*Correspondence: beki.manalie19@gmail.com

Received 15 April 2025; revised 07 May 2025; accepted 15 June 2025

Abstract

Intensified agriculture practices contribute to nutrient enrichment in freshwater lakes, causing eutrophication, algal blooms, and water hyacinth infestations. Eutrophication in Lake Tana, the source of the Blue Nile in Ethiopia, necessitates effective monitoring due to rapid infestation of water hyacinths. While traditional monitoring is costly and limited in spatial and temporal coverage, remote sensing offers a promising alternative. This study aims to develop a regression model to estimate Chlorophyll-a (Chl-a) concentration using in situ and remote sensing reflectance data. Field measurements from 143 locations across Lake Tana validated the correlation equations. Results show that the Moderate Resolution Imaging Spectroradiometer (MODIS) in near-infrared reflectance exhibits the strongest linear relationship with in situ Chl-a measurements for August 2016 ($R^2 = 0.53$), December 2016 ($R^2 = 0.56$) and March 2017 ($R^2 = 0.61$). The developed models were validated with a root-mean-square error of 2.76 µg/l, 5.89 µg/l, and 8.04 µg/l for August, December, and March, respectively. Applying the developed model from 2008–2018, the Chl-a concentration of the lake indicated an increasing trend, likely driven by non-point sources from surrounding watersheds, causing infestation of the lake by hyacinths since 2011. The agreement between MODIS and in situ Chl-a data, coupled with the satisfactory performance of the linear regression model, underscores that developing a regression model for Chl-a estimation from remote sensing in water hyacinth-infested lakes is a useful method in tracking spatiotemporal variations. This study will serve as a foundation for future Chl-a variation studies in Lake Tana and other similar lakes.

Keywords: Chlorophyll-a; estimation model; Lake Tana; MODIS; remote sensing; water hyacinth.

Introduction

Elevated Chl-a levels often indicate nutrient enrichment in freshwater lakes, causing eutrophication (Shi et al., 2022). This nutrient overloading, driven by anthropogenic impacts, can lead to harmful algal blooms, infestation of water hyacinths, oxygen depletion, and ecological imbalances (Palmer et al., 2015). While

effective management of Chl-a requires substantial data collection, the conventional Chl-a determination methods are always expensive and time-consuming. To address these limitations, utilizing remote sensing for water quality assessment has the potential to offer a highly effective solution (Bukata, 2013; Odermatt et al., 2012; Tyler et al., 2016). Integrating remote sensing data with limited conventional measurements can significantly enhance monitoring efforts in low-income countries. Remote sensing techniques offer a valuable means for monitoring Chl-a levels in freshwater lakes, providing comprehensive spatial and temporal data (Bresciani et al., 2011; Wang et al., 2022). However, not all satellite sensors are suitable for inland water quality monitoring. Satellites with coarse spatial resolution, regardless of their wide coverage, may not efficiently capture small inland water bodies. High resolution sensors, such as those on Sentinel-2 or Landsat 8, are well-suited for these applications (Pahlevan et al., 2019).

In recent years, numerous studies have demonstrated the effectiveness of satellite remote sensing data in mapping and estimating the distribution of Chl-a and water quality parameters in inland waters. Various types of satellite data, including Landsat TM, Landsat ETM+, Landsat-8, Moderate Resolution Imaging Spectroradiometer (MODIS), Medium Resolution Imaging Spectrometer (MERIS), Advanced Very High-Resolution Radiometer (AVHRR), SeaViewing Wide Field-of-view Sensor (SeaWiFS), and Satellite Pour l'Observation de la Terre (SPOT), have been used for this purpose (Womber et al., 2021). Therefore, remote sensing has become a vital tool for estimating Chl-a and water quality parameters globally (Fan et al., 2023; Yang et al., 2022). Furthermore, remote sensing's excellent spatial and temporal coverages make it a key tool in freshwater quality degradation due to the increasing population boom in developing countries (Adjovu et al., 2023; Sheffield et al., 2018).

Remote sensing studies about Chl-a retrieval in water proved an empirical relationship between radiance in bands or band ratios and observed Chl-a concentration (Moges et al., 2017; Wang et al., 2018; Wu et al., 2013). Early studies, such as Moges et al., (2017), utilized satellite-derived reflectance data from sensors like Landsat TM and ETM+ to estimate Chl-a concentrations in freshwater lakes. Their results indicated strong correlations when using band ratios involving blue and green wavelengths, enabling the development of regional-scale water quality monitoring algorithms. Constructing on this, Wang et al., (2024) employed hyperspectral remote sensing to evaluate coastal waters, emphasizing that narrow spectral bands in the red and near-infrared regions significantly enhanced the detection of phytoplankton-induced watercolor changes, particularly in optically complex waters.

Zheng et al. (2024) further examined the effectiveness of various band ratio algorithms across different aquatic environments, including lakes and reservoirs, confirming the reliability of empirical models when calibrated with extensive field measurements. They highlighted the significance of accounting for confounding factors such as suspended sediments and colored dissolved organic matter (CDOM), which can alter the reflectance signal captured by remote sensors, thereby introducing potential biases and errors in Chl-a concentration estimations if not properly considered. MODIS, known for its high temporal frequency, has been widely used for monitoring large lakes and reservoirs at regional to global scales. Its moderate spatial resolution, ranging between 250 and 1000 meters, allows for daily everyday observation of temporal dynamics in Chl-a concentration. However, the relatively coarse spatial resolution can limit precision for smaller water bodies (Ellis et al., 2024). Scholars often assimilate MODIS data with higher-resolution images from Landsat or Sentinel-2 to balance temporal and spatial resolution trade-offs (Ivanchuk et al., 2023).

Liu et al. (2010) developed a model to estimate Chl-a concentrations based on the ratio of near infrared (NIR) to red reflectance values, reporting a strong correlation with in-situ water sampling data ($R^2 = 0.85$) across a Chl-a concentration range of 5 to 60 mg/m^3. This NIR/red band ratio approach has since been applied in other studies, such as Papenfus et al. (2020), who used MODIS satellite imagery to estimate Chl-a concentrations in the Pearl River system. MODIS-Terra offers a higher temporal resolution and greater sensitivity compared to Landsat-7 ETM+ satellite images (Potapov et al., 2008). Additionally, satellite-

derived images of Chl-a can be obtained using single or combined band algorithms based on specific spectral regions of reflectance (Danbara, 2014; Kaba et al., 2014; Miller & McKee, 2004; Moges et al., 2017; Wang & Lu, 2010). Empirical, semi-empirical, and analytical models are commonly classified in studies (Caballero et al., 2022; Chang et al., 2022; Wang et al., 2018). Empirical models establish a direct relationship between apparent optical properties (such as remote sensing reflectance) and inherent optical properties (Chl-a) through statistical analyses like linear and nonlinear regression.

Information on remote sensing estimations of Chl-a is crucial for developing effective management strategies for algal blooms and water hyacinth infestations in many African lakes (Dube et al., 2015). The technology can potentially play a vital role, particularly in tackling large infestations, such as water hyacinths in unmanageably large shallow lakes such as Lake Tana, Ethiopia. The study, therefore, focuses on Lake Tana, Ethiopia, which is recently threatened by nutrient enrichment (Ateka, 2020; Tibebe et al., 2019; Moges et al., 2017), leading to a shift toward eutrophic conditions and water hyacinth infestations (Dersseh et al., 2022). The incidental occurrence and spread of water hyacinths since 2011 is attributed to the increased sediment and nutrient inflow into the lake (Dersseh et al., 2020), facilitated by the lake's circulation patterns (Kebedew et al., 2023).

Studies indicate that eutrophication driven by anthropogenic is the main cause for rapid spread of water hyacinth in Lake Tana (Mucheye et al., 2022). Since 2011, increasing pollution has contributed to frequent algal blooms and the spread of invasive water hyacinth in Lake Tana. A filed assessment conducted between May 15 and May 25, 2015, reported that the weed infested approximately 34,500 hectares of the lake (Anteneh et al., 2015) , although the exact area covered is debatable due to its dynamic nature. Water hyacinth poses serious threats to the environment, human health, and economic growth (Gezie et al., 2018). Social impacts include reduced access to clean water, a rise in waterborne diseases, displacement of communities, local conflicts, and limited access to water points. Ecologically, the infestation contributes to decreasing water quality, increased water loss due to high evapotranspiration, siltation, flooding, and a reduction in aquatic biodiversity (Dersseh, Melesse, et al., 2019). Infested areas are usually characterized by higher turbidity, elevated Chl-a concentrations, increased chemical oxygen demand (COD), and reduced levels of dissolved oxygen (DO), pH, and nitrates compared to non-infested areas (Mucheye et al., 2022).

Efficient monitoring of Chl-a concentrations is necessary to prevent further degradation of water quality (Markogianni et al., 2018). However, the traditional monitoring methods for Chl-a are cumbersome and time-consuming for large shallow lakes like Lake Tana (Wang et al., 2022). By leveraging remote sensing and improving the Chl-a retrieval model for the lake, Chl-a concentrations can be reliably estimated.

In Lake Tana, only a few studies have utilized remote sensing techniques to enable spatial and temporal observation of surface water parameters. The available previous research focused on the estimation of suspended sediment concentration distribution from MODIS-Terra satellite images over the whole lake body, calibrated by 20 in-situ observations (Wembera et al., 2021). Kaba et al. (2014) established a relationship between MODIS-Terra satellite images and sediment inflow from the Gumara River, which drains into Lake Tana from the east, and estimated sediment concentration loading over a 10 year periode (Kaba et al., 2014).Similarly, Landsat 7 ETM+ Images were also implemented for water quality trend analysis (Moges et al., 2017). Moges et al. (2017) investigated water clarity, dissolved phosphorus, and Chl-a concentration at a similar location to Kaba et al. (2014). All the above studies suffer from limited observation data for validating the developed models. Moreover, the two earlier studies, Kaba et al. (2014) and Moges et al. (2017), are concentrated on one inflow location of the lake, the Gumara inlet, which accounts for not more than 20% of the inflow to the lake (Kebede et al. 2006) which shows greater coverage is required.

Therefore, the objective of this study is to apply MODIS-Terra satellite reflectance to estimate Chl-a concentration over Lake Tana using observation data from 143 sampling locations at 5km grid locations sampled in August, December 2016 and March 2017. This study excels from previous Chl-a Landsat-based

estimations in Lake Tana, offering a robust comparison with observed data collected spatially covering the entire lake. Particularly, we aim to: (1) develop a linear regression model between in situ Chl-a concentrations and MODIS-Terra remote sensing reflectance, and (2) estimate the temporal variations in Chl-a concentrations over the lake. The research will provide a baseline to directly support the ongoing efforts by governmental and non-governmental organizations to eradicate water hyacinths from Lake Tana.

Materials and Methods

Study Area

Lake Tana, the headwaters of the Blue Nile, is located in the northwest of the Ethiopian plateaus (Figure 1). Geographically, the lake lies between 11°43'44" North, 37°23'22" East and 12°10'32" North, 37°15'08" East. As the largest freshwater resource in Ethiopia, Lake Tana holds about half of the country's fresh water reserve (McCartney et al., 2010) and covering 20% of the drainage area of the 15,096 km^2 Lake Tana basin (Setegn et al., 2011). The populations in the rural as well as those nearby towns are highly dependent on incomes from the lake economy, as it serves services such as transportation, hydropower, irrigation, fishing and ecotourism (Wondie, 2012).

The shallow lake with a mean depth of 9 m and a maximum depth of 15 m (Kebedew et al., 2020) is located in a wide depression of the Ethiopian basaltic plateau and is bordered by flood plains that are frequently flooded during the rainy season. These include the Fogera floodplain in the east (mainly by the Gumara and Rib rivers), Dembia floodplain in the north (from the Megech River), and Kunzila floodplain in the southwest (associated with Gilgel Abay, Kelti and Koga river). The Lake is bordered by steep rocks in the west and the northwest (McCartney et al., 2010). The lake is fed by more than 40 small streams (Kebede et al., 2006; Rientjes et al., 2011; Wale et al., 2009) and receives 93% of its volume from the major rivers of Gilgel Abay, Gumara, Ribb and Megech (Kebede et al. 2006). Usually, Shallow lakes are particularly susceptible to water quality impairment due to their limited water volume, high surface area to depth ratio, and enhanced interaction between sediments and the water column (Ayele & Atlabachew, 2021; Zhang et al., 2022). These physical characteristics increase their vulnerability to nutrient loading, sedimentation, and algal blooms (Kebedew et al., 2020). Lake Tana, the largest lake in Ethiopia, shares these shallow morphometric features and is therefore at risk of water quality deterioration. Similar issues have been observed in other Ethiopian lakes such as Ziway and Hawassa, where eutrophication has been driven by agricultural runoff, municipal wastewater discharge, and limited flushing capacity (Hailesilassie & Tegaye, 2019; Lencha et al., 2021).

The increasing sediment and nutrient loads from point sources in Bahir Dar town and non-point sources from the agricultural watersheds draining the lake contribute to the decline in water quality (McCartney et al., 2010). Due to agricultural intensification, land use change has occurred over time in the watershed (Biru et al., 2015) transported nutrients into the lake causes the overall water quality deterioration in Lake Tana (Dersseh et al., 2022). As a result, Lake Tana's trophic index level ranged from oligotrophic to hypereutrophic levels and the pollution index status ranged from slightly polluted to polluted annually (Nerae et al., 2024a). Moreover, the annual water quality indices ranged from good to very poor for ecological health and fair to unsuitable for drinking water, though the severity varied spatially and temporally, attributed to the inflow from the tributaries (Nerae et al., 2024b).

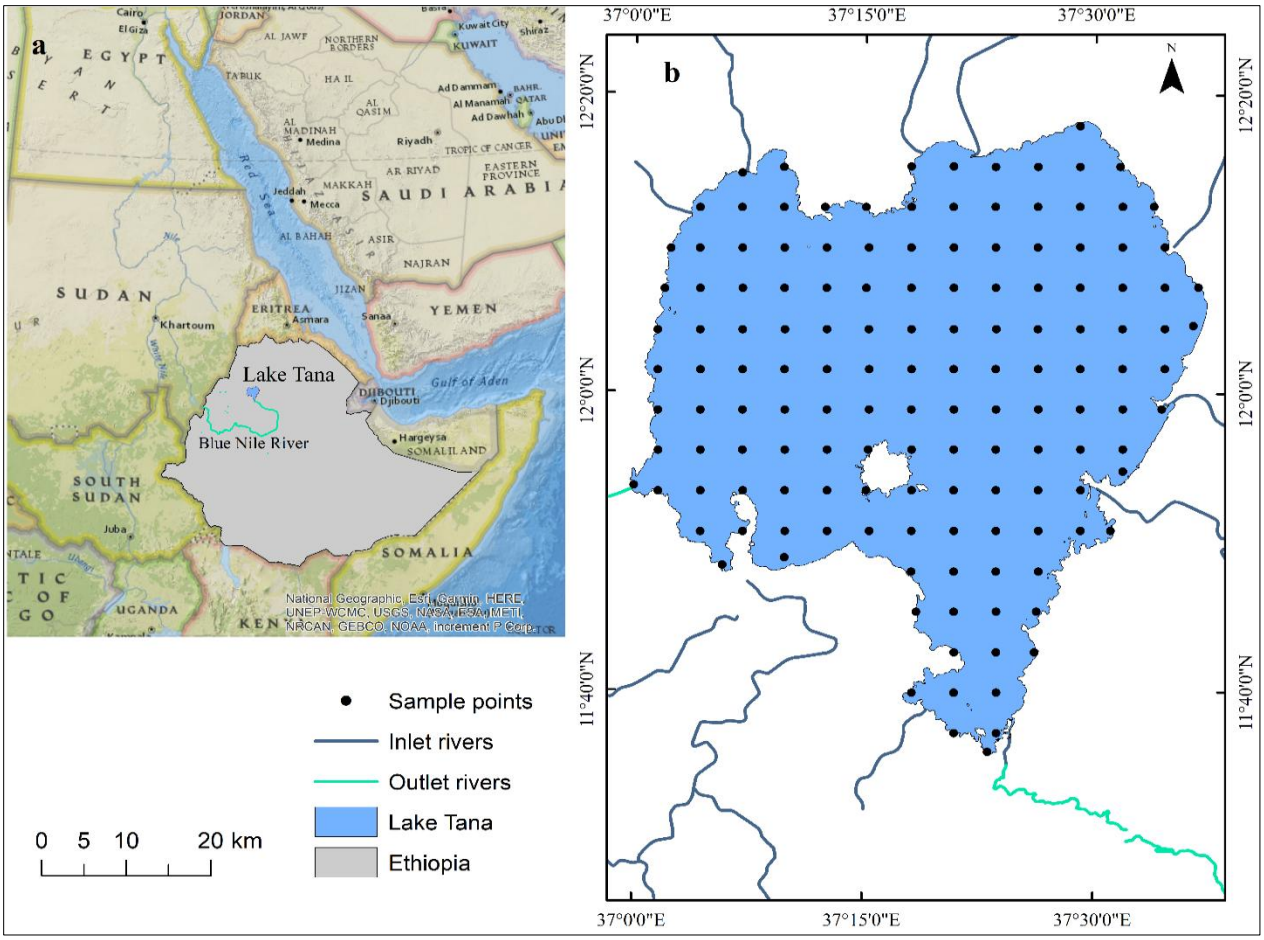

Fig. 1: Location map of the study area: (**a**) location map of Lake Tana and Ethiopia in the National Geographic World Map and, (**b**) Lake Tana indicating the sample point, inlet and outlet Rivers.

Chl-a Measurement

To determine the spatial and temporal variations of Chl-a measurements in Lake Tana, we used data collected by Atka (2020) and published by Dersseh et al. (2019). The data were collected from 143 sampling locations in the lake. Samples were collected three times, in August 2016, December 2016, and March 2017. The coordinates of the sampling locations were determined using a global positioning system (GPS) at a grid of 5km (Figure 1b). Chl-a concentration was determined from the water samples using an acetone extraction method. First, 100 mL of water was filtered through a glass fibre filter. The extract was then centrifuged and extracted overnight with 10 mL of 90% acetone in the dark at 4°C. Absorbance was measured at 750 and 664 nm before and after acidification. The absorbance at 750 nm was used to blank the absorbance at 664 nm. The absorbance at 664 nm was corrected for acidification by adding one hundred µL of 0.12 N HCl to the extract and waiting 60 seconds. The absorbance at 664 nm and 750 nm was then measured again. Purified Chl-a standards were run to calibrate the spectrophotometer. Chl-a concentration was calculated using the standard methods available in APHA (1998). Further details of the sampling protocol and laboratory determination are described in the cited materials.

MODIS Terra Data Acquisition and Preprocessing

MODIS data were selected for this study due to their high temporal resolution, long-term global coverage, and consistent data quality, which are important for Chl-a monitoring in dynamic inland and coastal waters. MODIS provides daily revisit capability, which greatly enhances the likelihood of obtaining usable, cloud-

free observations in regions frequently affected by cloud cover, particularly important when higher spatial resolution data (e.g., Sentinel-2 or Landsat) may have large temporal gaps due to clouds (Papenfus et al., 2020; Zhou et al., 2023).

While MODIS has a coarser spatial resolution (250–1000 m), it has proven effective for medium to large water bodies and long-term ecological studies due to its continuous data record since 2000 and its availability of critical bands (Red and NIR) for Chl-a estimation (Chen et al., 2025). Additionally, MODIS surface reflectance products include standard corrections for atmospheric effects and are extensively validated for aquatic remote sensing applications (Cao, Shen, et al., 2022; Pi et al., 2021; D. Wang et al., 2024) .

Recent studies continue to demonstrate the utility of MODIS for both empirical and semi-analytical models of Chl-a, especially in eutrophic, turbid, or optically complex waters where daily temporal frequency outweighs fine spatial detail (Johansen et al., 2022; Zhang et al., 2016). Moreover, MODIS data have been integrated successfully with machine learning and regression models to enhance prediction accuracy while maintaining operational feasibility (Li et al., 2023; Mohebzadeh et al., 2021). Thus, MODIS was chosen for its unique combination of temporal frequency, historical continuity, validated performance, and global accessibility, aligning with best practices in large-scale and long-term water quality monitoring.

Only the Red (620–670 nm) and Near-Infrared (NIR; 841–876 nm) bands from MODIS were extracted for this analysis because these spectral regions are highly responsive to Chl-a concentrations, particularly in inland and optically complex waters. Chl-a exhibits strong absorption in the red region due to its primary pigment characteristics, whereas the NIR region is dominated by scattering from algal cells and suspended particles (Cao, Shen, et al., 2022; Gitelson et al., 2011; Gurlin et al., 2011; Zhu et al., 2023). The selection of these bands is supported by their effectiveness in minimizing interference from colored dissolved organic matter (CDOM) and total suspended solids (TSS), which often affect shorter wavelengths.

Numerous studies have shown that the Red/NIR ratio or the NIR–Red difference correlates strongly with Chl-a, often outperforming blue-green band algorithms in turbid or eutrophic waters where colored dissolved organic matter (CDOM) and total suspended solids (TSS) interfere with reflectance at shorter wavelengths (Deng et al., 2024; Ha et al., 2013; Kolluru & Tiwari, 2022; Le et al., 2013). For example, Song et al. (2013) demonstrated the efficacy of both two-band (NIR/Red) and three-band (adding green) models for Chl-a estimation in diverse freshwater systems. Similarly, Yang et al. (2017) found that Red and NIR reflectance explained over 80% of the variation in Chl-a in productive lakes.

Compared to blue and green bands, which are often compromised by high concentrations of CDOM and suspended sediments (Greb et al., 2018; Ozbay et al., 2017), the Red–NIR spectral combination remains robust across a wide range of water quality conditions(Chen et al., 2025; Singh et al., 2013; Xia et al., 2024). Furthermore, Red and NIR bands are consistently available across major Earth observation satellites such as MODIS, Landsat, and Sentinel-2, facilitating inter-sensor comparisons and model transferability (Helder et al., 2018; Kganyago et al., 2023; Qin & Liu, 2022).

By focusing on these two bands, we developed a linear regression model to estimate Chl-a concentrations based on the strong empirical relationship between Red and NIR reflectance and in situ Chl-a measurements. This model leverages the absorption characteristics of Chl-a in the Red region and the scattering behavior in the NIR region, providing a robust, interpretable, and computationally efficient approach for monitoring optically complex inland and coastal waters(Huang et al., 2014; Leiger et al., 2020; Song et al., 2013; Yang et al., 2017).

For this study, we utilized the 250 m spatial resolution MODIS-Terra bands (Bands 1 and 2: Red and NIR) to estimate Chl-a concentrations in inland waters. To represent monthly reflectance, the median reflectance value was extracted for each sampled month during the data download process. The red and near-infrared (NIR) bands from the MODIS-Terra sensor were specifically selected due to their sensitivity to Chl-a and

their demonstrated effectiveness in monitoring optically complex inland waters (Cao, Shen, et al., 2022; Gupana et al., 2021; Raghul & Porchelvan, 2024). These data were acquired from the Google Earth Engine platform (https://code.earthengine.google.com) using custom JavaScript code developed to automate extraction for the specific sampling dates (Li et al., 2019).

To ensure the quality of the satellite data, we implemented a comprehensive multi-step quality assurance and quality control (QA/QC) protocol. First, we applied the MOD09Q1 product's QA flags to mask out pixels affected by clouds, shadows, and high aerosol concentrations, retaining only cloud-free observations (Hilker et al., 2012; Leinenkugel et al., 2013; Melchiorre et al., 2020; Zhang et al., 2024). Second, a land-water mask was applied to exclude non-aquatic pixels and minimize contamination from shoreline reflectance. To further reduce edge effects and spatial uncertainty, which are particularly important at 250 m resolution, we created a 500 m buffer around each in situ sampling location. Reflectance values were only averaged within this buffer if all pixels were cloud-free and classified as water, a method shown to improve the representativeness and spatial accuracy of satellite-derived measurements (Bishop-Taylor et al., 2019; Tottrup et al., 2022).

Specifically, the MODIS Terra surface reflectance product (MOD09Q1) was employed to estimate the Chl-a concentration in Lake Tana. Subsequently, using ArcGIS 10.8 spatial analysis tools, the reflectance values from the downloaded MOD09Q1 data were extracted at the precise in-situ sampling locations. In addition, we conducted visual inspections to identify and exclude pixels affected by sun glint, sensor striping, or atmospheric haze. Outlier reflectance values were also removed using thresholds established from validated inland water studies(Cao, Shen, et al., 2022; Feng et al., 2018). These QA/QC steps collectively ensured that the MODIS-Terra 250 m data used in our linear regression model were of high quality and suitable for accurately retrieving Chl-a concentrations in optically complex inland waters.

Retrieval Model of the Chl-a

A spectral index approach was employed to estimate Chl-a concentrations in lakes. Leveraging the bio-optical properties of Chl-a, various spectral indices, including band ratio, normalized difference, and single-band indices, were constructed (Table 1) (Wang et al., 2022). These indices, based on specific spectral band combinations, were designed to capture variations in Chl-a concentration. The optimal band combinations were identified by maximizing the Pearson correlation coefficient (R^2) between the calculated spectral indices and in situ Chl-a data. Subsequently, linear regression analysis was performed to establish a quantitative relationship between the selected MODIS bands and Chl-a concentrations. Finally, the derived linear regression models were applied to the MODIS imagery to generate Chl-a concentration maps for the lake.

Table 1: spectral indices for estimating Chl-a concentration.

Spectral indices	Calculation formula
Single Band index	$\mathrm{Chl-a} = \mathrm{A} + \mathrm{B} * \rho\mathrm{i}$
Ratio Band index	$\mathrm{Chl-a} = \mathrm{C} + \mathrm{D} * \frac{\rho\mathrm{i}}{\rho\mathrm{j}}$
Normalized difference index	$\mathrm{Chl-a} = \mathrm{E} + \mathrm{F} * \frac{\rho\mathrm{i}-\rho\mathrm{j}}{\rho\mathrm{i}+\rho\mathrm{j}}$

where A, B, C, D, E and F are the correlation coefficients of the regression model, and ρi and ρj (i, j = B1 and B2) are the water reflectance of two bands selected by the MODIS data sources.

Chl-a Retrieval and Assessment Methods

To retrieve Chl-a concentrations, a linear regression model was developed using selected spectral features derived from MODIS-Terra data. Feature importance was assessed through Pearson correlation coefficients with in-situ Chl-a measurements. Between the tested variables, NIR reflectance shown the strongest correlation ($R^2 = 0.53$), compared to NDVI ($R^2 = 0.46$), the Simple Ratio ($R^2 = 0.42$), and red reflectance

(R^2 = 0.23). The results show that NIR reflectance is the best informative predictor of Chl-a concentration in Lake Tana. The Chl-a concentration was retrieved through linear fitting based on the MODIS surface reflectance data and in situ measured Chl-a concentration data. Additional, the root-mean-square error (RMSE), mean absolute error (MAE) and mean absolute percentage error (MAPE) were used to evaluate the accuracy of the Chl-a retrieval results.

There is no fixed RMSE threshold for chl-a remote sensing accuracy; tolerable values depend on trophic status, use, and data variability. In the mesotrophic to eutrophic lakes like Lake Tana, RMSEs of 2–10 µg/L are mostly tolerable if they continue below 30% of the mean Chl-a concentration(Assegide et al., 2023; Makwinja et al., 2023; Shahvaran, 2024). This level of precision usually provisions consistent revealing of spatial and seasonal patterns. Conversely, further stringent precision (lower RMSE) may be essential for operational monitoring. The smaller the MAE value is, the closer the retrieval value is to the real value. The MAPE is the average absolute percentage error, where a MAPE value of 0% means a perfect model and a MAPE greater than 100% means an inferior model. The equations can be expressed according to (Cao, Ma, et al., 2022).

$$\mathrm{RMSE} = \sqrt{\frac{1}{n}\sum_{i=1}^{n}(Y_i - X_i)^2} \quad (1)$$

$$\mathrm{MAE} = \frac{1}{n}\sum_{i=1}^{n}|Y_i - X_i| \quad (2)$$

$$MAPE = \frac{1}{n}\sum_{i=1}^{n}\left|\frac{Y_i - X_i}{Y_i}\right| \times 100\% \quad (3)$$

where n represents the number of observed values, and X_i and Y_i represent the retrieval value and true value of the Chl-a, respectively.

Calibration and Validation of regression models

Following the methodology outlined by (Álvarez Robles, 2019), the predictive performance of the final regression model was evaluated using independent calibration and validation datasets. The dataset was randomly divided into two groups: 70% of the data was designated for calibration, to develop the linear regression model. The remaining 30% of the data served as the validation dataset, used to assess the accuracy of the regression coefficients derived from the calibration process.

Statistical Methods

To assess trends in Chl-a, the non-parametric Mann–Kendall trend test (Kendall, 1948; Mann, 1945) was applied to determine whether a statistically significant trend existed in the time series data over the 2008–2018 period. The time series plot of Chl-a concentration over Lake Tana for August, December, and March, based on satellite image from 2008–2018, is presented. The Mann–Kendall nonparametric trend test analyzes the sign of the difference between later-year data and earlier-year data. The Mann–Kendall test examines whether there is a monotonic upward or downward trend in the dataset, meaning the values consistently increase or decrease over time. It works by evaluating the sign of differences between pairs of observations, comparing later data points to earlier ones. The number of positive differences versus negative differences determines the direction and strength of the trend. Normalized test statistics, Z are computed according to (Douglas et al., 2000). The size of the statistical variable Z represents the change in the trend of the data. The significance level (α) is set to be 0.05, under which the $Z_{1-\alpha/2}$ equals 1.96. When $|Z| \geq Z_{1-\alpha/2}$, the hypothesis is not accepted in a two-sided test. Flowingly, $Z > 0$ indicates a positive trend, while $Z < 0$ indicates a negative trend.

Results

Observed Chl-a concentrations

The Chl-a concentration were measured at 143 sampling locations across Lake Tana. The average Chl-a concentration increased markedly from 2.2 µg/L (ranging from 0.1 to 19.4 µg/L) in August 2016, to 13.6 µg/L (ranging from 0.1 to 148.2 µg/L) in December 2016, and reaching a peak of 21.4 µg/L (ranging from 0.1 to 191.6 µg/L) in March 2017 (Table 2 and Table S1 in the supplemental material). Both the mean and the range of Chl-a values show a distinct seasonal progression, with the lowest concentrations occurring during the rainy season (August) and the highest concentrations during the dry season (March).

Spatially, Chl-a concentrations in August exhibited two distinct zones , with minimum values on the western side and maximum values on the eastern side of Lake Tana (Figure 2a). In December, the highest concentrations appeared in the southeastern and northeastern regions, while the western part still had the lowest concentrations (Figure 2b). The lowest concentration in December extended to the majority of the northern part and limited areas in the east. Conversely, during the dry season in March, the spatial distribution had completely changed, showing the lowest concentrations in the south, northeast, northwest, and certain parts of the central lake, while the maximum concentrations were observed in the north, east at the entrance of the Gumara River, and southwest at the entrance of the Gilgel Abay River (Figure 2c).

Table 2: Descriptive statistics for the measured Chl-a concentrations of Lake Tana in µg/L

Aug 2016, Chl-a (µg/L)	Dec 2016, Chl-a (µg/L)	Mar 2017, Chl-a (µg/L)
Mean	2.2	13.6	21.4
Median	1.3	4.0	12.7
Standard Deviation	2.8	26.7	27.1
Range	19.3	148.1	191.5
Minimum	0.1	0.1	0.1
Maximum	19.4	148.2	191.6
Confidence Level (95%)	0.5	4.4	4.5

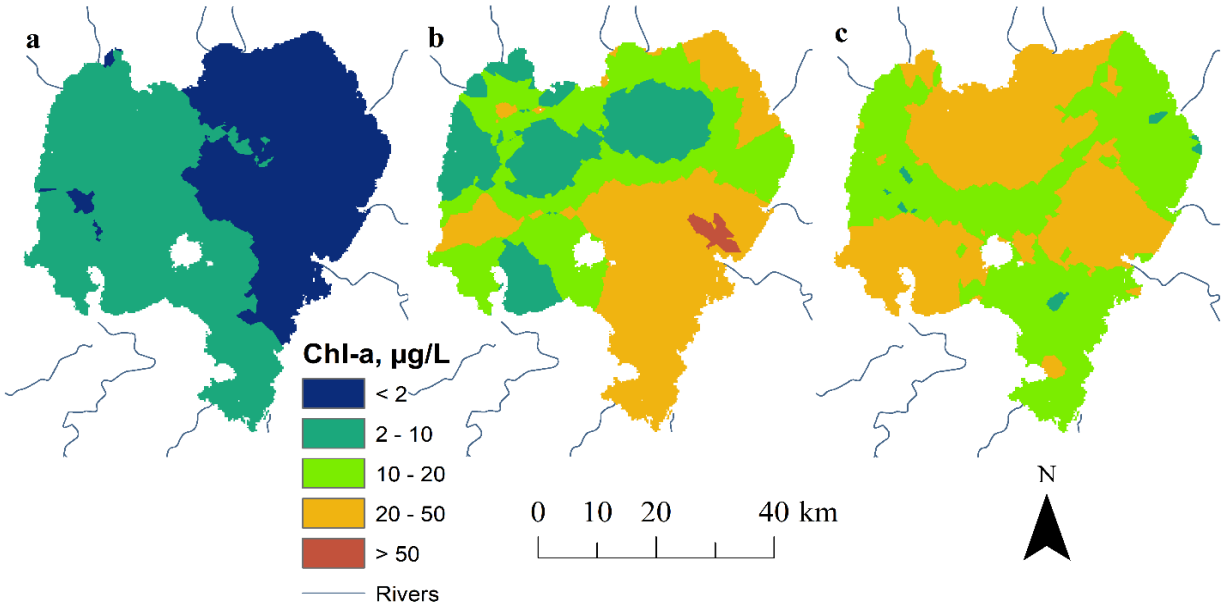

Fig 2: Measured Chl-a concentrations in µg/L of Lake Tana on: (**a**) August 2016; (**b**) December 2016, and (**c**) March 2017

Correlation between Estimated and Measured Chl-a Concentrations

Predicted Chl-a concentrations exhibited a clear seasonal trend, increasing substantial from August to March in alignment with the observed data. Specifically, predicted Chl-a values followed a parallel trajectory, starting at 2.86 µg/L in August, progressing to 15.35 µg/L in December, and reaching a maximum of 21.75 µg/L in March, as detailed in Tables 2, 3 and Table S2 in the supplemental material. This upward trend indicates a maximum concentration during the dry season, suggesting a strong influence of seasonal factors on algal growth. The prediction accuracy evaluated with RMSE and MAE was within a reasonable range (Table 3).

Table 3: Descriptive statistics for the measured Vs. Estimated Chl-a concentrations in µg/L.

Date	Mean measured Chl-a (µg/L)	Mean estimated Chl-a (µg/L)	Max	Min	SD	RMSE	MAE	MAPE
22-31Aug-2016	2.2	2.86	6.85	0.0	1.87	2.76	0.42	12.50%
14-22 Dec-2016	13.6	15.34	157.40	0.0	26.11	5.89	0.90	3.13%
14-23 Mar-2017	21.4	21.75	58.16	0.0	12.03	8.04	1.23	6.80%

A consistent linear relationship was identified between Chl-a concentrations and various combinations of red and near-infrared (NIR) bands derived from MODIS-Terra reflectance data. Notably, the NIR band exhibited the highest correlation, proving most effective for Chl-a retrieval across all sampling periods . Consequently, specific regression equations were developed for each sampling period. For August 2016, the calibrated relationship between Chl-a and MODIS-Terra reflectance is represented by equation (4), visually depicted in Figure 2. Similarly, equations (5) and (6) detail the calibrated regression relationships for December 2016 and March 2017, respectively.

$$Chl - a = -38.75 * \rho NIR + 8.18, for\ R^2 = 0.53, n = 100\ and\ p < 0.001 \quad (4)$$

$$Chl - a = 1001.7 * \rho NIR - 13.19, for\ R^2 = 0.56, n = 100, and\ p < 0.001 \quad (5)$$

$$Chl - a = -606.3 * \rho NIR + 68.56, for\ R^2 = 0.61\ , n = 100, and\ p < 0.001 \quad (6)$$

where *Chl-a* is expressed in *µg/L*, n is the number of samples, p indicates a statistically significant probability of the linear relationship ($p < 0.001$), and R^2 represents the coefficient of determination, quantifying the goodness of fit for August (Table 3 and Figure 2), for December (Table S3 and Figure S1 in the supplemental material), and for March (Table S4 and Figure S2 in the supplemental material).

Table 3: Estimation statistics for various band combinations; bold numbers have the largest R^2, in August 2016.

Band combinations*	R^2	Adjusted R^2	Standard error	Significance F
Red	0.23	0.22	0.96	0.0000
NIR	**0.53**	**0.52**	**0.75**	**0.0000**
Red+NIR	0.43	0.42	0.83	0.0000
Red-NIR	0.17	0.16	0.99	0.0000
NIR/Red	0.42	0.41	0.83	0.0000
NDVI (red-NIR/red+NIR)	0.46	0.46	0.8	0.0000

*The band explaining the best relationship with the Chl-a has the highest R^2 and lowest standard error, which is indicated in bold.

The correlation analysis confirmed a significant relationship between MODIS near-infrared (NIR) band reflectance and Chl-a concentration, though the strength of this correlation varied across different months, as evidenced by the fluctuating R^2 values in equations (4-6). Notably, the R^2 values demonstrated that the MODIS NIR band effectively predicts Chl-a concentrations. Furthermore, equations (5) and (6) provide the model coefficients necessary to calculate Chl-a levels across the entire surface of Lake Tana, utilizing the pixel reflectance values from the satellite imagery. The statistical significance of these correlations was confirmed by p-values consistently below 0.05 ($P < 0.05$).

Figure 3 illustrates the relationship between MODIS spectral bands and Chl-a concentrations, revealing that the near-infrared (NIR) band is the most effective for Chl-a retrieval in Lake Tana. The scatter plot in Figure 3 and supplementary Figures S1 & S2 show a clear linear relationship between NIR band reflectance and Chl-a levels, confirming its suitability for accurate estimation. In contrast, the red band showed minimal correlation, suggesting it is not informative for water quality retrieval in this context. This finding underscores the importance of the NIR band in MODIS for detecting Chl-a. Furthermore, the MODIS-derived Chl-a estimates exhibited a statistically significant correlation ($R^2 = 0.53$) with observed values, and a Root Mean Squared Error (RMSE), Mean Absolute Error (MAE), and Mean Absolute Percentage Error (MAPE) at a p-value less than 0.005. These results collectively demonstrate that MODIS, particularly utilizing the NIR band, can effectively detect and estimate Chl-a concentrations in these inland waters.

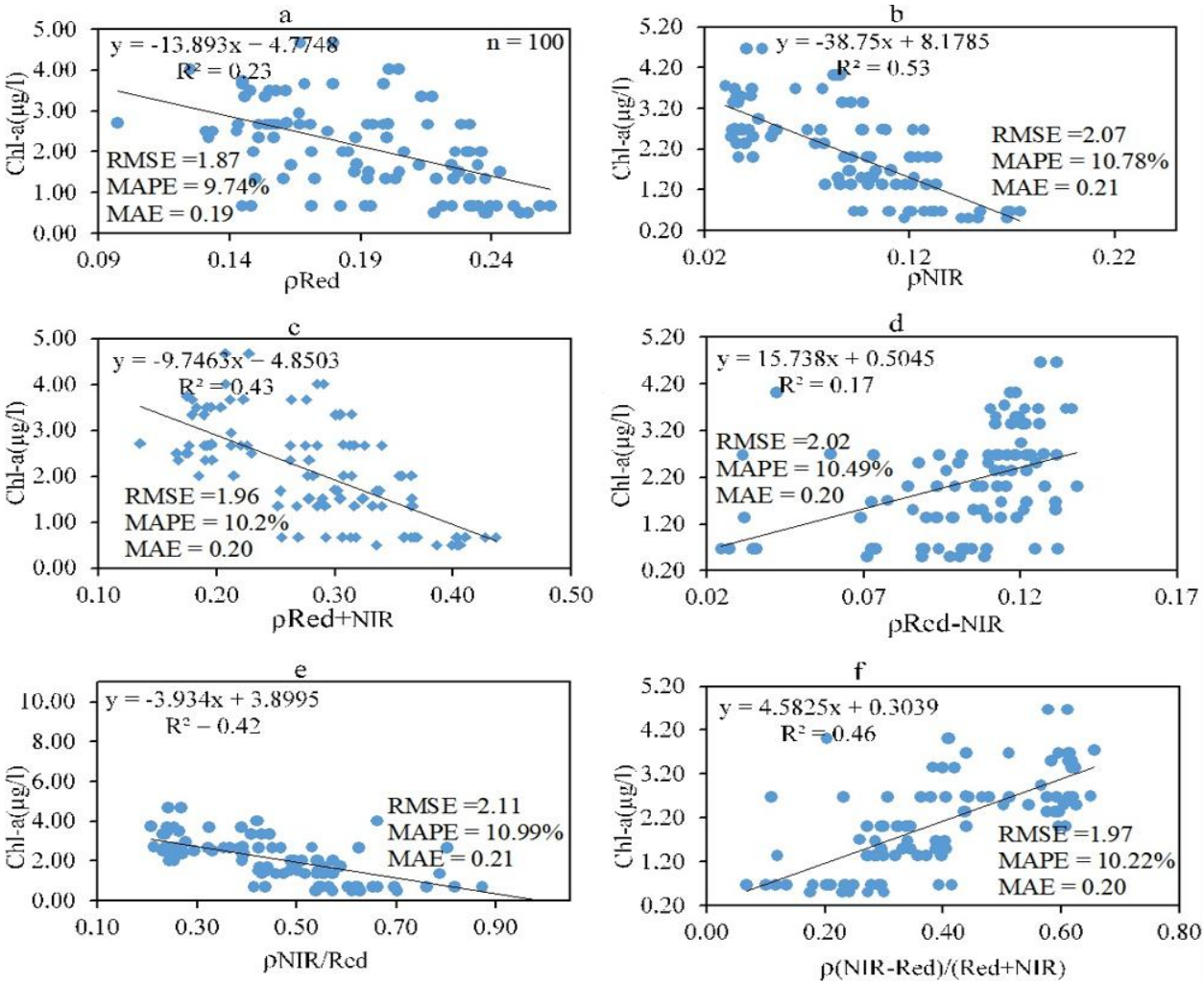

Fig. 3: Scatter plot of observed Chl-a (µg/L) against Mod 09 Q1 surface reflectance bands in August 2016.

Predicted Ch-a Distribution of Lake Tana

The predicted results revealed clear spatiotemporal variation in Chl-a concentration over Lake Tana across the observed months. The predicted Chl-a concentration averaged 2.86 µg/L in August 2016, with values ranging from 0 to 6.9 µg/L. In December 2016, the average increased to 15.35 µg/L, with values ranging of 0 to 157.4 µg/L. Through March 2017, Chl-a reached an average of 21.75 µg/L, ranging from 0 to 58.6 µg/L (Tables 3 & S2).

Figure 4 illustrates a consistent spatially increasing trend in Chl-a concentrations from August to March. In August, the lowest values were observed in the western part of Lake Tana, with higher concentrations in the east (Figure 4a). In December, the highest levels were recorded at the entrance of the main rivers (Figure 4b). In March, Chl-a concentrations were generally elevated throughout the lake.

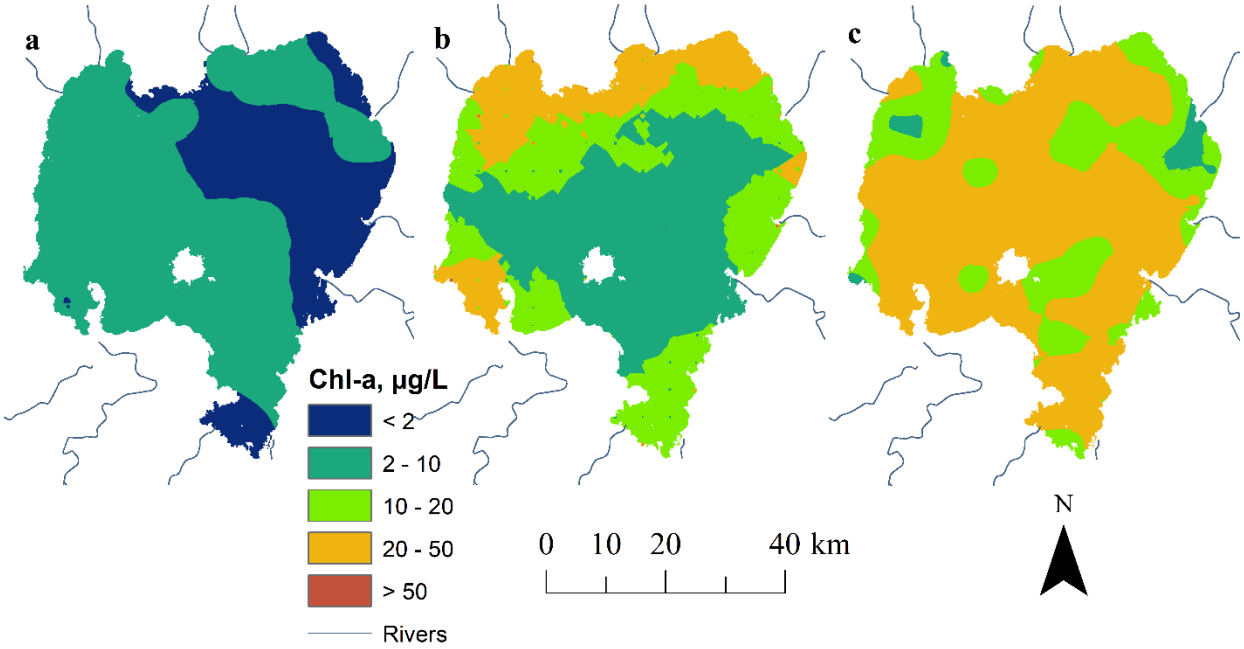

Fig. 4: Retrieval of the Chl-a concentrations in Lake Tana on: (**a**) August 2016; (**b**) December 2016 and (**c**) March 2017

Generating Chl-a time series data for Lake Tana

Using the developed regression equations, the Chl-a concentrations were retrieved over a 10 year period (2008-2018). The spatial distribution of Chl-a concentrations was then mapped to visualize the spatial variations of each year for the predicted months (Figures S3, S4 and S5). Retrieved Chl-a concentration in the lake for August 2016, December 2016, and March 2017 showed an increasing trend from the 2008 to 2018 periods (Figure 5). As the computed p-value is lower than the significance level alpha (0.05), the null hypothesis was rejected, and the alternative hypothesis was accepted in favor of the increasing trend in the series, particularly during the dry seasons.

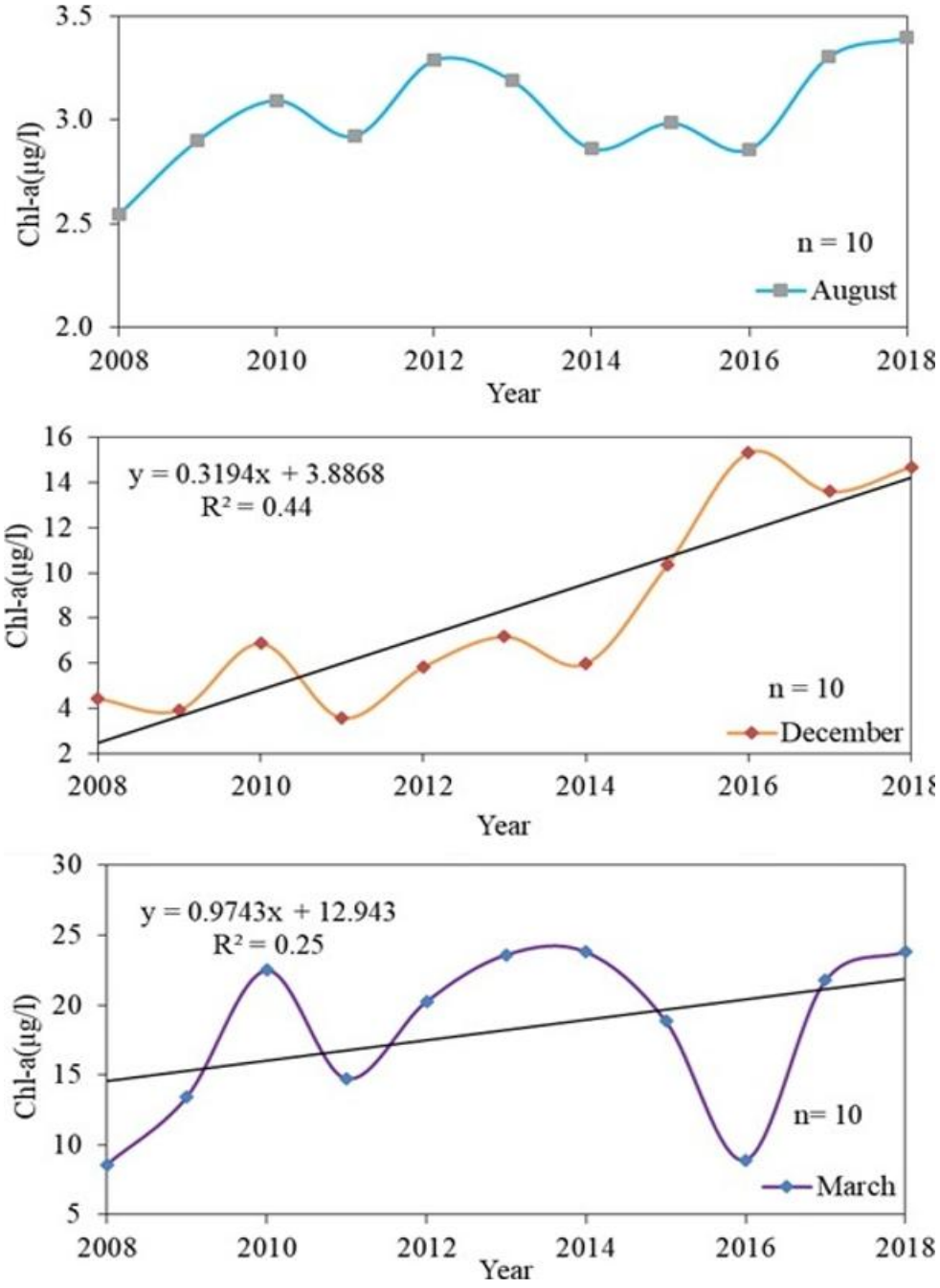

Fig. 5: Estimated Chl-a time series (2008–2018) for Lake Tana, derived from the developed model.

From the 10 -year period, the R^2 values from the linear trend analyses indicate a weak to moderate link among the variables used to estimation of Chl-a concentrations. The R^2 values of 0.43, 0.44, and 0.25 propose that the linear models described simply 25% to 44% of the variation in Chl-a over period. This indicates that, while some temporal trends have existed, a substantial portion of the variability residues unexplained, probably caused by the effect of other environmental or anthropogenic factors not captured by the linear models.

Discussion

Spatiotemporal Chl-a Patterns

This study utilized MODIS/Terra Surface Reflectance 8-Day L3 data to estimate Chl-a concentrations in Lake Tana, which is seriously infested with water hyacinth. Chl-a concentrations resulting from satellite data were validated using in situ samples collected from 143 locations. A linear regression model applied to the red and near-infrared bands, with a spatial resolution of 250 m, achieved an R^2 of 0.53, RMSE of 2.76 µg/L, MAE of 0.42 µg/L, and MAPE of 12.5%. These metrics suggest that the model captures a significant portion of the spatial variability in Chl-a of the lake.

The performance of this study aligns with Gidudu et al.(2021) showed R^2 values of up to 0.80 and RMSE around 5 µg/L in Lake Victoria, the largest African lake, using empirical models with MODIS data. Studies such as Oliveira Santos et al. (2024) indicated that MODIS 500 m products yield R^2 values between 0.60 and 0.75 for Chl-a in Brazilian reservoirs, with RMSE values from 2 to 4 µg/L, comparable with this study's results. In contrast, advanced performance was noted in studies, for example Feng et al. (2018) and Zhang et al. (2016) where R^2 exceeded 0.85 and RMSE was below 0.4 µg/L; However, these studies often targeted less turbid waters.

MODIS-based model accuracy differs broadly based on the waterbody type, optical complexity, resolution of imagery, and choice of algorithm (Table 4). Such comparisons for Chl-a estimation in various inland and coastal water bodies highlight both the reliability of the current study's results with the broader literature and the challenges of remote sensing in complex lake systems like Lake Tana.

Table 4: Comparative summary of error metrics from studies using MODIS data for chl-a estimation in inland and coastal waters.

Study	Dataset Used	Model	R^2	RMSE	MAE
This Study	MODIS (250m)	Linear Regression	0.53	2.76 µg/L	0.42 µg/L
Moges et al. (2017)	Landsat 7 ETM+	Non-Linear Regression	0.45	—	—
Wu et al. (2009)	MODIS& Landsat TM5	Multiple Regression	0.88	0.37 m	—
Li et al. (2019)	MODIS	Multiple Linear Regression		3.2 µg/L	0.51 µg/L
Zhang et al. (2022)	MODIS + Ground Data	Random Forest	0.61	2.9 µg/L	—
McCullough et al. (2012)	MODIS (250 m)	Multiple Regression	0.85	0.34 m	—
Feng et al. (2018)	MODIS	Empirical Model	0.9	0.25 µg/L	—
Han et al. (2022)	MODIS & Field Data	Semi-Empirical Models	Varies	Varies	—
Zhang et al. (2021)	MODIS	Empirical Modeling	Up to 0.80	Around 5 µg/L	—
Oliveira Santos et al. (2024)	MODIS (500 m)	Product Performance Analysis	0.60–0.75	2–4 µg/L	—
Abbas et al. (2019)	MODIS	GROC4 Algorithm	—	—	—

The viability and accuracy of regression models for Chl-a estimation are often season-dependent, as the optical properties of water bodies vary throughout the year. For example, Kallio et al. (2001) confirmed that model coefficients derived for May differ noticeably from those for August, reflecting seasonal variations in water composition and light conditions. Similarly, Chl-a coefficients for August vary from those obtained in December and March. The spectral signal of Chl-a is notably weak in environments with high suspended material concentrations, which is a common condition in Lake Tana during the rainy and post-rainy periods (Ayele & Atlabachew, 2021). Furthermore, the surface extent and optical properties of Lake Tana's water fluctuate significantly across seasons, influenced by rainfall and sediment load (Kebedew et al., 2021; Seong et al., 2017).

Emerging research continues to emphasize the impact of seasonal variations on Chl-a estimation. For instance, Cao et al. (2022) observed that Chl-a concentrations in small lakes were higher in summer and autumn compared to spring and winter, with air temperature positively correlating with seasonal mean Chl-a across various lake sizes. Similarly, Ngamile et al. (2025) found that Chl-a concentrations strongly absorbed light in the blue (490 nm) and red (665 nm) wavelengths, while reflecting light in the green (560 nm) and near-infrared (842 nm) wavelengths, with significant seasonal variations in these spectral characteristics. Studies leveraging MODIS data have significantly advanced our understanding of seasonal variability in Chl-a concentrations across various aquatic systems (Devi and Sarangi (2023) Harid et al. (2022) Harid et al. (2022) Sun et al. (2023); Ye et al. (2024).

The seasonal dynamics of Chl-a concentrations in Lake Tana are closely associated with climatic conditions, particularly during the dry season when increased sunshine hours and wind-induced resuspension of nutrients encourage higher rates of phytoplankton growth (Kebedew et al. (2021). As underlined by Moges et al. (2017), Chl-a tends to increase during the dry period due to enhanced solar radiation. Our findings also revealed a consistent increase in Chl-a concentrations from August to March (Figure 5), a pattern commonly attributed to phytoplankton blooms encouraged by prolonged sunlight exposure. This seasonal blooming is further facilitated by the resuspension of particulate nutrients from the lake bed, mainly driven by wind-induced mixing, as noted by Kebedew et al. (2021).

Besides natural drivers, anthropogenic activities significantly influence Chl-a concentrations. While Lake Tana is a vulnerable water body, runoff from adjacent farmlands, especially during the dry season, introduces fertilizer-derived nutrients into the lake, promoting eutrophication (Alemu et al., 2017). Recent studies, such as Nerae et al. (2024), confirm that nutrient-rich runoff continues to be a major contributor to algal growth in Lake Tana. This nutrient enrichment, if unconstrained, can cause more severe algal blooms and a decline in water quality.

Comparatively, Moges et al. (2017) used Landsat 7 ETM+ and non-linear regression to estimate Chl-a, reporting an average value of 3.76 µg/L in December, lower than our current findings using MODIS 8-Day L3. This variation may be due to differences in satellite resolution, the spectral range of sensors, or seasonal variability in nutrient dynamics. Additionally, current literature highlights the growing effectiveness of MODIS based methods for Chl-a retrieval. For instance, Zhang et al. (2024) confirmed that MODIS temporal granularity enables better alignment with in-situ observations, particularly under conditions of variable cloud cover. Also, studies by Devi and Sarangi (2023) and (Deng et al., 2017) have revealed the reliability of MODIS data in tracking phytoplankton dynamics in tropical and subtropical freshwater systems. These results and Table 4 confirm the utility of MODIS 250 m imagery for consistent, cost-effective, and large-scale monitoring of water quality parameters such as Chl-a, particularly in dynamic freshwater systems like Lake Tana, where seasonal and anthropogenic influences interrelate.

Temporally, the Chl-a concentration predicted by the linear regression model for 2016 exhibited notable seasonal variability. The maximum predicted concentration reached 157.4 µg/L in December, 2016 while

the minimum was 0 µg/L in August (Figure 4). This wide range of predicted values exceeded the observed in situ measurements (Table 2), showing that the model tended to overestimate the peak Chl-a levels by approximately 9.2 µg/L in December, 2016 and underestimate the lower extremes, such as in August, 2016 and March, 2017 where observed values were 0.05 µg/L and 133 µg/L, respectively. These inconsistencies highlight limitations of the linear regression model, particularly its reduced capacity to capture nonlinear dynamics and extreme fluctuations commonly seen in complex inland waters (Gidudu et al., 2021).

This pattern aligns with findings by Mucheye et al. (2022), who used Sentinel imagery to estimate Chl-a in Lake Tana and reported a maximum value of 40.0 µg/L by the end of August, with a minimum of 4.41 µg/L in June. Their study emphasizes that the peak Chl-a concentration tends to occur during the post-rainy season, rather than during peak rainfall months, likely due to nutrient influx from catchment runoff. Similarly, Wondie et al. (2007) observed that the highest spatial coverage of Chl-a also occurred after the rainy season, rather than during it, further emphasizing the delayed response of phytoplankton growth to nutrient input.

Comparatively, models using Landsat 7 ETM+ satellite data have also shown seasonal performance variability. Moges et al. (2017) found that the model underperformed during transitional months like November 2014 and May, 2015 with R^2 values of just 0.28 and 0.11, respectively. Regardless of these model performance issues, the average Chl-a concentration predicted by the MODIS based regression model in our study remained comparable to the in situ observed mean (Table 2), suggesting that while extreme values are poorly captured, the model is reasonably effective for estimating average concentrations. Despite that recent literature further supports the need for seasonally adaptive or non-linear models to improve accuracy in predicting Chl-a in dynamic lakes (Zhang et al., 2024 ; (Deng et al., 2024).

Another latest finding by Nerae et al. (2024a) in Lake Tana revealed that the lowest concentration of Chl-a was observed in the rainy season due to reduced algal blooms from increased rainfall, wind waves, diminished light, and higher dilution caused by new runoff (Nerae et al., 2024a; Kebedew et al., 2023). The highest levels of Chl-a were found in the post-rainy and dry seasons and were attributed to ample light, stagnant water, biochemical changes, and enhanced phytoplankton growth. Therefore, our predictions of Chl-a concentration appear to be more accurate than those who predicted the highest Chl-a coverage during the rainy period (Mucheye et al., 2022). Alike the current study, recent research showed that the Rib and Gumara inlets (eastern parts) and Gilgel Abay River (western parts) of the lake have higher nutrient influxes and amplify Chl-a levels (Kebedew et al., 2023; Nerae et al., 2024). This is attributed to wind-driven circulation patterns in the lake, which result in extended residence times for pollutants entering through different inlets (Kebedew et al., 2023). Most of the previous studies on Lake Tana indicated that the lake water quality was impaired (Melaku et al., 2020; Tibebe et al., 2019). According to Nerae et al. (2024a) Lake Tana is identified to be in a middle-eutrophic to hypereutrophic state, with considerable nutrient fluxes contributing to algal blooms, which further cause degraded water quality (Nerae et al., 2024). Thus, this study shows that Chl-a concentrations in Lake Tana are very high, confirming that the lake is Eutrophic, complementing the Nerae et al. (2024) study.

When comparing the Chl-a levels in Lake Tana with other African lakes, we found that Chl-a concentration measured from the two largest Ethiopian Rift Valley lakes in Ethiopia, Lake Abaya and Lake Chamo, between 2016 and 2019 ranged from 17.0 ± 3.6 µg/L in Lake Abaya to 33.0 ± 11.6 µg/L in Lake Chamo (Dagne et al., 2023) is slightly lower with this study which ranges from 2.24 to 21.75 µg/L. A similar study in Victoria Lake using in situ Chl-a and MODIS satellite images showed poor performance (R^2=0.03) compared to our study (R^2 = 0.53) (Gidudu et al., 2021). In the case of Lake Malawi, Chl-a concentration estimations from MODIS surface reflectance were very low, ranging from 0.05 µg/L to 0.27 µg/L, with a mean value was 1.0 µg/L, verifying that the lake was oligotrophic during this time (Chavula et al., 2009). In Lake Naivasha, Kenya, using MODIS surface reflectance, the maximum and minimum values of Chl-a concentration varied from 0 µg/L in January to 40 µg/L in December. According to Ndungu et al., (2013),

MODIS satellite data tend to underestimate Chl-a concentrations compared to in-situ measurements. However, in this study, both under and overestimation occurred. Similar variability has been noted in other regions. For instance, Han and Jordan (2005) reported Chl-a concentrations ranging from 0.93 to 24.92 µg/L in Pensacola Bay using Landsat ETM+, while Rani et al., (2019) found values between 3.22 and 3.41 µg/L in Ghana's Densu River using Landsat-8. However, Chl-a concentrations in Lake Tana were higher than the above-stated lakes and rivers compared with the maximum value.

Elevated Chl-a levels in Lake Tana can likely be attributed to increased nutrient inputs resulting from expanding agricultural activities within the lakes catchment (Worqlul et al., 2020; Alemu et al., 2017), a pattern similarly observed in other Ethiopian lakes . For example, Lake Chamo showed Chl-a concentrations of 19.64 to 33.28 µg/L largely due to runoff from agricultural fertilizers and resident wastewater (Admas et al., 2020; Goshu & Aynalem, 2017; Tesfaye, 2023; Wondie, 2009). Likewise, Lake Ardibo exhibited strong periodic discrepancy influenced by ecological drivers (Mohammed et al., 2023). Studies from external Ethiopia as well support this pattern: eutrophic conditions allied to land use were detected in Lake Qilu, China (Li et al., 2022), and high Chl-a variability was recognized in Lake Chad (Buma & Lee, 2020) and Hulun Lake (Zhang et al., 2024). These results collected highlight the significance of land use practices, nutrient loading, and hydrological dynamics in inducing Chl-a variability through various freshwater systems.

Overall, Lake Tana suffered major water quality changes over time (Nerae et al., 2024b; Dersseh et al., 2022). Accurate predictions help decision-makers understand the full extent of water quality degradation in the lake. For example, since 2003, the average spatial Chl-a concentration has increased from 4.8µg/L, according to (Wondie et al., 2007), to 32.7 µg/L in 2020. Thus, there has been an eight-fold increase in Chl-a within just two decades. Our study confirms (Nerae et al., 2024) and Dersseh et al. (2022) by demonstrating a decline in Lake Tana's water quality, shifting from slightly polluted to polluted, driven by eutrophication, evidenced by water hyacinth proliferation, and attributed to nutrient enrichment, oxygen depletion, and elevated suspended solids, with significant impacts observed in coastal areas (Kebedew et al., 2021). For future research, it is necessary to develop a refined algorithm with some additional in situ measurements and expand the study to assess the impact of various best management practices on water quality. While this study does not exhaustively explore all empirical formula models, the relationship established with remote sensing variables would provide insight into the factors affecting the Chl-a variable. In general, the linear regression model developed can be applied as a tool to reduce costs and efforts in fieldwork measures and to understand eutrophication in this lake transition ecosystem.

Implications for the Evolution of Water Hyacinths and Eutrophication

Several reports have been published regarding the external nutrient loads and water quality status of Lake Tana, (Alemu et al., 2020; Ewnetu et al., 2014; Tibebe et al., 2019), ecological condition and the coverage of water hyacinth (Dersseh, Kibret, et al., 2019; Wondie, 2018), algal bloom and trophic status of the lake (Moges et al., 2017; Tibebe et al., 2019; Wondie, 2018), and pollution and eutrophication level (Nerae et al., 2024). The Chl-a results found in the current assessment are linked to the surface water quality and eutrophication status of the lake, indicated by different authors including (Alemu et al., 2020; Ayele & Atlabachew, 2021; Dersseh, Melesse, et al., 2019; Nerae et al., 2024). The main factors influencing the growth and spread of water hyacinth include total nitrogen, phosphorus levels, pH, surface water temperature, salinity, and water depth (Gaikwad & Gavande, 2017). According to previous studies (Alemu et al., 2020; Ayele & Atlabachew, 2021; Dersseh, Melesse, et al., 2019), the north and northeastern parts of Lake Tana are highly susceptible to water hyacinth invasion, which aligns with the current Chl-a spatial pattern. Moreover, the studies indicate that shallower areas of the lake tend to have a higher presence of water hyacinth, which is closely linked to the current levels of higher Chl-a concentrations at those shoreline regions. Collectively, these papers have highlighted a decline in water quality, an increase in water hyacinth, and eutrophication over time. These changes may be related to non-point source pollution,

sediment and nutrient inflows, and elevated erosion rates from the watershed, particularly due to agricultural activities (Alemu et al., 2020; Moges et al., 2017).

Nutrient inflows, particularly phosphorus concentrations, are the most significant factors contributing to the growth of water hyacinths in Lake Tana (Dersseh, Kibret, et al., 2019; Worqlul et al., 2020). The accumulation of sediment and phosphorus from the northern and eastern catchments of Lake Tana is a primary contributor to the high levels of suspended sediment and the reduced visibility measured by the Secchi disk (Kebedew et al., 2023). In the northern and eastern regions of Lake Tana, increased phosphorus concentrations and turbidity lead to reduced light transparency and shorter Secchi disk readings. This phenomenon is directly related to elevated Chl-a concentrations and the process of eutrophication (Nerae et al., 2024)2024a). The increase in Chl-a, eutrophication, and water hyacinth proliferation is particularly evident when water levels decline, especially during the dry seasons (Dersseh, Kibret, et al., 2019; Dersseh, Melesse, et al., 2019; Kebedew et al., 2021; Kebedew et al., 2020). Given the significant accumulation of phosphorus in the sediment, managing and curbing the spread of water hyacinths in Lake Tana is likely to be a lengthy and complex process (Admas et al., 2020). Since phosphorus cycles from the bottom sediment to the water hyacinths, which accumulate in their biomass (Kebedew et al., 2023). Harvesting these plants could help lower the phosphorus concentration in the sediment.

In addition, the trophic status of Lake Tana has been evaluated at various times (Moges et al., 2017; Nerae et al., 2024; Tibebe et al., 2019) using the Carlson Trophic State Index to assess the lake's condition. Their findings indicated that Lake Tana's trophic state falls between mesotrophic and hypereutrophic. Furthermore, they noted that Chl-a concentration was directly linked to the level of eutrophication, with higher Chl-a levels found in the shoreline areas of Lake Tana, especially during the dry monsoon season, where the trophic status was elevated. The external loading of nutrients and agrochemicals from the watershed surrounding the lake, primarily through the four major rivers during the wet season, is considered a key factor exacerbating Chl-a levels and eutrophication in the lake. To improve the current algal biomass in terms of Chl-a and trophic status, it is recommended to implement wetland management, reduce recession agriculture, manage agrochemical use in the watershed, and establish buffer zones around the lake.

Conclusion

Eutrophication, often signaled by elevated Chl-a levels due to excess nutrients, is difficult to assess in large lakes using traditional methods. Remote sensing offers a potential solution. In this study, we validated MODIS-Terra daily remotely sensed Chl-a concentrations against 143 observed measurements collected from a large, shallow lake characterized by water hyacinth infestation. The results showed that the NIR band based on the MODIS image presented the best performance for estimating Chl-a in Lake Tana. The variation of Chl-a concentration over the lake was associated with the seasonal variation of the regional climate. Chl-a concentration is greatest in the dry season and is lower in the rainy season. A strong statistical relationship was observed between Chl-a concentration and MODIS-Terra daily reflectance over Lake Tana. The constructed linear regression model was used to estimate the Chl-a concentration time series for 10 years, and it was found that the highest concentration of Chl-a has an increasing trend, deteriorating the water quality of Lake Tana. The reasonable agreement between MODIS and in situ Chl-a data, together with favorable results from the linear regression model where ecologically important parameters were also included, reveals the applicability and necessity of further studies on estimating Chl-a, from satellite imagery in the area. Overall, the spatial patterns of Chl-a concentrations in Lake Tana’s coastal areas were higher than in the pelagic areas, likely due to higher nutrient and pollutant inputs from agricultural activities of the surrounding and upstream areas. Seasonally, the lowest concentration of Chl-a was observed in the rainy monsoon, associated with reduced wind waves, algal blooms, increased rainfall, diminished light, and higher dilution caused by new runoff. The highest levels of Chl-a were recorded during the dry monsoons period, when increased temperature, ample light, stagnant water, and biochemical changes

promote phytoplankton growth. The research establishes a foundation for directly aiding scholars in their ongoing fight to eradicate water hyacinths from Lake Tana, Ethiopia, and other similar African lakes. Continued refinement of remote sensing models and incorporation of additional ecological variables will further enhance water quality monitoring and inform sustainable lake management practices.

Author Contributions

B.W.A. contributed to conceptualization, data collection and analysis, writing the first draft, and incorporating feedback from co-authors. F.A.Z. contributed to research objectives, and methodologies, and provided overall supervision of the research work. M.G.K. helped in reviewing, structuring the paper, and rewriting the initial draft. S.T. and M.D.N. provided valuable feedback through manuscript restructuring, review and editing. All the authors declare that they reviewed the manuscript and accepted the published paper.

Data Availability Statement

The data used for the research are available from the first author upon request (beki.manalie19@gmail.com).

Conflicts of Interest

The authors have declared no conflict of interest.

References

Adjovu, G. E., Stephen, H., James, D., & Ahmad, S. (2023). Overview of the application of remote sensing in effective monitoring of water quality parameters. *Remote Sensing*, *15*(7), 1938.

Admas, A., Sahile, S., Agidie, A., Menale, H., Gedefaw, T., & Teshome, M. (2020). Controlling water hyacinth infestation in Lake Tana using Fungal pathogen from Laboratory level upto pilot scale. *bioRxiv*, 2020.2001. 2014.901140.

Alemu, M. L., Worqlul, A. W., Zimale, F. A., Tilahun, S. A., & Steenhuis, T. S. (2020). Water balance for a tropical lake in the volcanic highlands: Lake Tana, Ethiopia. *Water*, *12*(10), 2737.

Álvarez Robles, E. J. (2019). Supervised Learning models with ice hockey data. In.

Assegide, E., Shiferaw, H., Tibebe, D., Peppa, M. V., Walsh, C. L., Alamirew, T., & Zeleke, G. (2023). Spatiotemporal Dynamics of Water Quality Indicators in Koka Reservoir, Ethiopia. *Remote Sensing*, *15*(4), 1155.

Ayele, H. S., & Atlabachew, M. (2021). Review of characterization, factors, impacts, and solutions of Lake eutrophication: lesson for lake Tana, Ethiopia. *Environmental Science and Pollution Research*, *28*(12), 14233-14252.

Biru, M. K., Minale, A. S., & Debay, A. B. (2015). Multitemporal land use land cover change and dynamics of Blue Nile Basin by using GIS and remote sensing techniques, north-western Ethiopia. *Int. J. Environ. Sci*, *4*(2), 81-88.

Bishop-Taylor, R., Sagar, S., Lymburner, L., Alam, I., & Sixsmith, J. (2019). Sub-pixel waterline extraction: Characterising accuracy and sensitivity to indices and spectra. *Remote Sensing*, *11*(24), 2984.

Bukata, R. P. (2013). Retrospection and introspection on remote sensing of inland water quality:" Like Déjà Vu All Over Again". *Journal of Great Lakes Research*, *39*, 2-5.

Buma, W. G., & Lee, S.-I. (2020). Evaluation of sentinel-2 and landsat 8 images for estimating chlorophyll-a concentrations in lake Chad, Africa. *Remote Sensing*, *12*(15), 2437.

Caballero, C. B., Guedes, H. A. S., ANDRADE, A. C. F., Martins, V. S., Fraga, R. S., & Mendes, K. G. (2022). Empirical and semi-empirical chlorophyll-a modeling for water quality assessment through river-lake transition in extreme Southern Brazil. *Anais da Academia Brasileira de Ciências*, *94*.

Cao, Z., Ma, R., Melack, J. M., Duan, H., Liu, M., Kutser, T., Xue, K., Shen, M., Qi, T., & Yuan, H. (2022). Landsat observations of chlorophyll-a variations in Lake Taihu from 1984 to 2019. *International Journal of Applied Earth Observation and Geoinformation*, *106*, 102642.

Cao, Z., Shen, M., Kutser, T., Liu, M., Qi, T., Ma, J., Ma, R., & Duan, H. (2022). What water color parameters could be mapped using MODIS land reflectance products: A global evaluation over coastal and inland waters. *Earth-Science Reviews*, *232*, 104154.

Chang, F., Hou, P., Wen, X., Duan, L., Zhang, Y., & Zhang, H. (2022). Seasonal stratification characteristics of vertical profiles and water quality of Lake Lugu in Southwest China. *Water*, *14*(16), 2554.

Chavula, G., Brezonik, P., Thenkabail, P., Johnson, T., & Bauer, M. (2009). Estimating chlorophyll concentration in Lake Malawi from MODIS satellite imagery. *Physics and Chemistry of the Earth, Parts A/B/C*, *34*(13-16), 755-760.

Chen, L., Liu, L., Liu, S., Shi, Z., & Shi, C. (2025). The Application of Remote Sensing Technology in Inland Water Quality Monitoring and Water Environment Science: Recent Progress and Perspectives. *Remote Sensing*, *17*(4), 667.

Danbara, T. T. (2014). *Deriving water quality indicators of Lake Tana, Ethiopia, from Landsat-8* University of Twente].

Deng, Y., Zhang, Y., Li, D., Shi, K., & Zhang, Y. (2017). Temporal and spatial dynamics of phytoplankton primary production in Lake Taihu derived from MODIS data. *Remote Sensing*, *9*(3), 195.

Deng, Y., Zhang, Y., Pan, D., Yang, S. X., & Gharabaghi, B. (2024). Review of recent advances in remote sensing and machine learning methods for lake water quality management. *Remote Sensing*, *16*(22), 4196.

Dersseh, M. G., Ateka, A., Zimale, F. A., Worqlul, A. W., Moges, M. A., Dagnew, D. C., Tilahun, S. A., & Melesse, A. M. (2020). Dynamics of eutrophication and its linkage to water hyacinth on lake Tana, upper Blue Nile, Ethiopia: understanding land-lake interaction and process. Advances of Science and Technology: 7th EAI International Conference, ICAST 2019, Bahir Dar, Ethiopia, August 2–4, 2019, Proceedings 7,

Dersseh, M. G., Kibret, A. A., Tilahun, S. A., Worqlul, A. W., Moges, M. A., Dagnew, D. C., Abebe, W. B., & Melesse, A. M. (2019). Potential of water hyacinth infestation on lake Tana, Ethiopia: a prediction using a GIS-based multi-criteria technique. *Water*, *11*(9), 1921.

Dersseh, M. G., Melesse, A. M., Tilahun, S. A., Abate, M., & Dagnew, D. C. (2019). Water hyacinth: review of its impacts on hydrology and ecosystem services—lessons for management of Lake Tana. *Extreme hydrology and climate variability*, 237-251.

Dersseh, M. G., Steenhuis, T. S., Kibret, A. A., Eneyew, B. M., Kebedew, M. G., Zimale, F. A., Worqlul, A. W., Moges, M. A., Abebe, W. B., & Mhiret, D. A. (2022). Water quality characteristics of a water hyacinth infested tropical highland lake: Lake Tana, Ethiopia. *Frontiers in Water*, *4*, 774710.

Devi, K. N., & Sarangi, R. (2023). Monitoring of monthly scale chlorophyll concentration variability in the Bay of Bengal and Arabian Sea using MODIS Aqua Satellite Data. *Journal of Geomatics*, *17*(1), 1-10.

Douglas, E., Vogel, R., & Kroll, C. (2000). Trends in floods and low flows in the United States: impact of spatial correlation. *Journal of hydrology*, *240*(1-2), 90-105.

Ellis, E. A., Allen, G. H., Riggs, R. M., Gao, H., Li, Y., & Carey, C. C. (2024). Bridging the divide between inland water quantity and quality with satellite remote sensing: An interdisciplinary review. *Wiley Interdisciplinary Reviews: Water*, *11*(4), e1725.

Ewnetu, D. A., Bitew, B. D., & Chercos, D. H. (2014). Determination of surface water quality status and identifying potential pollution sources of Lake Tana: particular emphasis on the lake boundary of Bahirdar City, Amhara region, north west Ethiopia, 2013. *J Environ Earth Sci*, *4*(13), 88-97.

Fan, W., Xu, Z., Dong, Q., Chen, W., & Cai, Y. (2023). Remote sensing-based spatiotemporal variation and driving factor assessment of chlorophyll-a concentrations in China's Pearl River Estuary. *Frontiers in Marine Science*.

Feng, L., Hu, C., & Li, J. (2018). Can MODIS land reflectance products be used for estuarine and inland waters? *Water Resources Research*, *54*(5), 3583-3601.

Gaikwad, R. P., & Gavande, S. (2017). Major factors contributing growth of water hyacinth in natural water bodies. *International Journal of Engineering Research*, *6*(6), 304-306.

Gidudu, A., Letaru, L., & Kulabako, R. N. (2021). Empirical modeling of chlorophyll a from MODIS satellite imagery for trophic status monitoring of Lake Victoria in East Africa. *Journal of Great Lakes Research*, *47*(4), 1209-1218.

Gitelson, A. A., Gurlin, D., Moses, W. J., & Yacobi, Y. Z. (2011). Remote estimation of chlorophyll-a concentration in inland, estuarine, and coastal waters. In (pp. 449-478): Taylor and Francis Group, Boca Raton, Florida.

Goshu, G., & Aynalem, S. (2017). Problem overview of the lake Tana basin. *Social and ecological system dynamics: Characteristics, trends, and integration in the Lake Tana Basin, Ethiopia*, 9-23.

Greb, S., Dekker, A. G., Binding, C., Bernard, S., Brockmann, C., DiGiacomo, P., Griffith, D., Groom, S., Hestir, E., & Hunter, P. (2018). *Earth observations in support of global water quality monitoring*. International Ocean-Colour Coordinating Group.

Gupana, R. S., Odermatt, D., Cesana, I., Giardino, C., Nedbal, L., & Damm, A. (2021). Remote sensing of sun-induced chlorophyll-a fluorescence in inland and coastal waters: Current state and future prospects. *Remote sensing of Environment*, *262*, 112482.

Gurlin, D., Gitelson, A. A., & Moses, W. J. (2011). Remote estimation of chl-a concentration in turbid productive waters—Return to a simple two-band NIR-red model? *Remote sensing of Environment*, *115*(12), 3479-3490.

Ha, N. T. T., Koike, K., & Nhuan, M. T. (2013). Improved accuracy of chlorophyll-a concentration estimates from MODIS imagery using a two-band ratio algorithm and geostatistics: As applied to the monitoring of eutrophication processes over Tien Yen Bay (Northern Vietnam). *Remote Sensing*, *6*(1), 421-442.

Hailesilassie, W. T., & Tegaye, T. A. (2019). Comparative Assessment of the Water Quality Deterioration of Ethiopian Rift Lakes: The Case of Lakes Ziway and Hawassa. *Environmental & Earth Sciences Research Journal*, *6*(4).

Harid, R., Demarcq, H., & Houma, F. (2022). SeaSonal trend decompoSition of modiS chlorophyll biomaSS timeS SerieS in the algerian baSin. *Geo-Eco-Marina*, *28*, 41-47.

Helder, D., Markham, B., Morfitt, R., Storey, J., Barsi, J., Gascon, F., Clerc, S., LaFrance, B., Masek, J., & Roy, D. P. (2018). Observations and recommendations for the calibration of Landsat 8 OLI and Sentinel 2 MSI for improved data interoperability. *Remote Sensing*, *10*(9), 1340.

Hilker, T., Lyapustin, A. I., Tucker, C. J., Sellers, P. J., Hall, F. G., & Wang, Y. (2012). Remote sensing of tropical ecosystems: Atmospheric correction and cloud masking matter. *Remote sensing of Environment*, *127*, 370-384.

Huang, C., Zou, J., Li, Y., Yang, H., Shi, K., Li, J., Wang, Y., Chena, X., & Zheng, F. (2014). Assessment of NIR-red algorithms for observation of chlorophyll-a in highly turbid inland waters in China. *ISPRS Journal of Photogrammetry and Remote Sensing*, *93*, 29-39.

Ivanchuk, N., Kogut, P. I., & Martyniuk, P. (2023). Sentinel-2 and MODIS Data Fusion for Generation of Daily Cloud-Free Images at the Sentinel Resolution Level. COLINS (3),

Johansen, R. A., Reif, M. K., Saltus, C. L., & Pokrzywinski, K. L. (2022). A review of empirical algorithms for the detection and quantification of harmful algal blooms using satellite-borne remote sensing.

Kaba, E., Philpot, W., & Steenhuis, T. (2014). Evaluating suitability of MODIS-Terra images for reproducing historic sediment concentrations in water bodies: Lake Tana, Ethiopia. *International Journal of Applied Earth Observation and Geoinformation*, *26*, 286-297.

Kebede, S., Travi, Y., Alemayehu, T., & Marc, V. (2006). Water balance of Lake Tana and its sensitivity to fluctuations in rainfall, Blue Nile basin, Ethiopia. *Journal of hydrology*, *316*(1-4), 233-247.

Kebedew, M. G., Tilahun, S. A., Belete, M. A., Zimale, F. A., & Steenhuis, T. S. (2021). Sediment deposition (1940–2017) in a historically pristine lake in a rapidly developing tropical highland region in Ethiopia. *Earth Surface Processes and Landforms*, *46*(8), 1521-1535.

Kebedew, M. G., Tilahun, S. A., Zimale, F. A., Belete, M. A., Wosenie, M. D., & Steenhuis, T. S. (2023). Relating Lake Circulation Patterns to Sediment, Nutrient, and Water Hyacinth Distribution in a Shallow Tropical Highland Lake. *Hydrology*, *10*(9), 181.

Kebedew, M. G., Tilahun, S. A., Zimale, F. A., & Steenhuis, T. S. (2020). Bottom sediment characteristics of a tropical lake: Lake Tana, Ethiopia. *Hydrology*, *7*(1), 18.

Kendall, M. G. (1948). Rank correlation methods.

Kganyago, M., Ovakoglou, G., Mhangara, P., Adjorlolo, C., Alexandridis, T., Laneve, G., & Beltran, J. S. (2023). Evaluating the contribution of Sentinel-2 view and illumination geometry to the accuracy of retrieving essential crop parameters. *GIScience & Remote Sensing*, *60*(1), 2163046.

Kolluru, S., & Tiwari, S. P. (2022). Modeling ocean surface chlorophyll-a concentration from ocean color remote sensing reflectance in global waters using machine learning. *Science of the Total Environment*, *844*, 157191.

Le, C., Hu, C., Cannizzaro, J., English, D., Muller-Karger, F., & Lee, Z. (2013). Evaluation of chlorophyll-a remote sensing algorithms for an optically complex estuary. *Remote sensing of Environment*, *129*, 75-89.

Leiger, K., Linnanto, J. M., & Freiberg, A. (2020). Establishment of the Q y Absorption Spectrum of Chlorophyll a Extending to Near-Infrared. *Molecules*, *25*(17), 3796.

Leinenkugel, P., Kuenzer, C., & Dech, S. (2013). Comparison and enhancement of MODIS cloud mask products for Southeast Asia. *International Journal of Remote Sensing*, *34*(8), 2730-2748.

Lencha, S. M., Tränckner, J., & Dananto, M. (2021). Assessing the water quality of lake Hawassa Ethiopia—trophic state and suitability for anthropogenic uses—applying common water quality indices. *International journal of environmental research and public health*, *18*(17), 8904.

Li, D., Chang, F., Wen, X., Duan, L., & Zhang, H. (2022). Seasonal variations in water quality and algal blooming in hypereutrophic Lake Qilu of southwestern China. *Water*, *14*(17), 2611.

Li, F., Yigitcanlar, T., Nepal, M., Nguyen, K., & Dur, F. (2023). Machine learning and remote sensing integration for leveraging urban sustainability: A review and framework. *Sustainable Cities and Society*, *96*, 104653.

Li, H., Wan, W., Fang, Y., Zhu, S., Chen, X., Liu, B., & Hong, Y. (2019). A Google Earth Engine-enabled software for efficiently generating high-quality user-ready Landsat mosaic images. *Environmental modelling & software*, *112*, 16-22.

Liu, Y., Guo, H., & Yang, P. (2010). Exploring the influence of lake water chemistry on chlorophyll a: A multivariate statistical model analysis. *Ecological modelling*, *221*(4), 681-688.

Makwinja, R., Inagaki, Y., Sagawa, T., Obubu, J. P., Habineza, E., & Haaziyu, W. (2023). Monitoring trophic status using in situ data and Sentinel-2 MSI algorithm: lesson from Lake Malombe, Malawi. *Environmental Science and Pollution Research*, *30*(11), 29755-29772.

Mann, H. B. (1945). Nonparametric tests against trend. *Econometrica: Journal of the econometric society*, 245-259.

Markogianni, V., Kalivas, D., Petropoulos, G. P., & Dimitriou, E. (2018). An appraisal of the potential of Landsat 8 in estimating chlorophyll-a, ammonium concentrations and other water quality indicators. *Remote Sensing*, *10*(7), 1018.

McCartney, M., Alemayehu, T., Shiferaw, A., & Awulachew, S. (2010). *Evaluation of current and future water resources development in the Lake Tana Basin, Ethiopia* (Vol. 134). IWMI.

Melaku, A., Yalew, A., Hailu, B., & Yitayew, T. (2020). Current Trophic Status of Lake Tana, Ethiopia. *Livestock Research Results*, 522.

Melchiorre, A., Boschetti, L., & Roy, D. P. (2020). Global evaluation of the suitability of MODIS-Terra detected cloud cover as a proxy for Landsat 7 cloud conditions. *Remote Sensing*, *12*(2), 202.

Miller, R. L., & McKee, B. A. (2004). Using MODIS Terra 250 m imagery to map concentrations of total suspended matter in coastal waters. *Remote sensing of Environment*, *93*(1-2), 259-266.

Moges, M. A., Schmitter, P., Tilahun, S. A., Ayana, E. K., Ketema, A. A., Nigussie, T. E., & Steenhuis, T. S. (2017). Water quality assessment by measuring and using landsat 7 ETM+ images for the current and previous trend perspective: lake tana Ethiopia. *Journal of Water Resource and Protection*, *9*(12), 1564.

Mohammed, A., Mengistou, S., & Fetahi, T. (2023). The effects of water quality parameters, water level changes, and mixing on zooplankton community dynamics in a tropical high-mountain Lake Ardibo, Ethiopia. *Environmental Monitoring and Assessment*, *195*(8), 927.

Mohebzadeh, H., Mokari, E., Daggupati, P., & Biswas, A. (2021). A machine learning approach for spatiotemporal imputation of MODIS chlorophyll-a. *International Journal of Remote Sensing*, *42*(19), 7381-7404.

Mucheye, T., Haro, S., Papaspyrou, S., & Caballero, I. (2022). Water quality and water hyacinth monitoring with the Sentinel-2A/B satellites in Lake Tana (Ethiopia). *Remote Sensing*, *14*(19), 4921.

Nerae, M. D., Kebedew, M. G., Abebe, B. A., Moges, M. A., Zimale, F. A., Asres, B. W., & Steenhuis, T. S. (2024). Assessment of pollution and trophic state of a water hyacinth infested tropical highland lake: Lake Tana in Ethiopia. *Sustainable Water Resources Management*, *10*(5), 1-15.

Ngamile, S., Madonsela, S., & Kganyago, M. (2025). Trends in remote sensing of water quality parameters in inland water bodies: a systematic review. *Frontiers in Environmental Science*, *13*, 1549301.

Odermatt, D., Gitelson, A., Brando, V. E., & Schaepman, M. (2012). Review of constituent retrieval in optically deep and complex waters from satellite imagery. *Remote sensing of Environment*, *118*, 116-126.

Oliveira Santos, V., Guimarães, B. M. D. M., Neto, I. E. L., de Souza Filho, F. d. A., Costa Rocha, P. A., Thé, J. V. G., & Gharabaghi, B. (2024). Chlorophyll-a estimation in 149 tropical semi-arid reservoirs using remote sensing data and six machine learning methods. *Remote Sensing*, *16*(11), 1870.

Ozbay, G., Fan, C., & Yang, Z. (2017). Relationship between land use and water quality and its assessment using hyperspectral remote sensing in mid-atlantic estuaries. In *Water Quality*. IntechOpen.

Pahlevan, N., Chittimalli, S. K., Balasubramanian, S. V., & Vellucci, V. (2019). Sentinel-2/Landsat-8 product consistency and implications for monitoring aquatic systems. *Remote sensing of Environment*, *220*, 19-29.

Palmer, S. C., Kutser, T., & Hunter, P. D. (2015). Remote sensing of inland waters: Challenges, progress and future directions. In (Vol. 157, pp. 1-8): Elsevier.

Papenfus, M., Schaeffer, B., Pollard, A. I., & Loftin, K. (2020). Exploring the potential value of satellite remote sensing to monitor chlorophyll-a for US lakes and reservoirs. *Environmental Monitoring and Assessment*, *192*(12), 808.

Pi, X., Feng, L., Li, W., Liu, J., Kuang, X., Shi, K., Qi, W., Chen, D., & Tang, J. (2021). Chlorophyll-a concentrations in 82 large alpine lakes on the Tibetan Plateau during 2003–2017: temporal–spatial variations and influencing factors. *International Journal of Digital Earth*, *14*(6), 714-735.

Potapov, P., Hansen, M. C., Stehman, S. V., Loveland, T. R., & Pittman, K. (2008). Combining MODIS and Landsat imagery to estimate and map boreal forest cover loss. *Remote sensing of Environment*, *112*(9), 3708-3719.

Qin, R., & Liu, T. (2022). A review of landcover classification with very-high resolution remotely sensed optical images—Analysis unit, model scalability and transferability. *Remote Sensing*, *14*(3), 646.

Raghul, M., & Porchelvan, P. (2024). A Critical Review of Remote Sensing Methods for Inland Water Quality Monitoring: Progress, Limitations, and Future Perspectives. *Water, Air, & Soil Pollution*, *235*(2), 159.

Rientjes, T., Perera, B., Haile, A., Reggiani, P., & Muthuwatta, L. (2011). Regionalisation for lake level simulation–the case of Lake Tana in the Upper Blue Nile, Ethiopia. *Hydrology and Earth System Sciences*, *15*(4), 1167-1183.

Setegn, S. G., Rayner, D., Melesse, A. M., Dargahi, B., & Srinivasan, R. (2011). Impact of climate change on the hydroclimatology of Lake Tana Basin, Ethiopia. *Water Resources Research*, *47*(4).

Shahvaran, A. R. (2024). *Chlorophyll-a Mapping in a Large Lake Using Remote Sensing Imagery: A Case Study of Western Lake Ontario* University of Waterloo].

Sheffield, J., Wood, E. F., Pan, M., Beck, H., Coccia, G., Serrat-Capdevila, A., & Verbist, K. (2018). Satellite remote sensing for water resources management: Potential for supporting sustainable development in data-poor regions. *Water Resources Research*, *54*(12), 9724-9758.

Shi, J., Shen, Q., Yao, Y., Li, J., Chen, F., Wang, R., Xu, W., Gao, Z., Wang, L., & Zhou, Y. (2022). Estimation of chlorophyll-a concentrations in small water bodies: comparison of fused Gaofen-6 and Sentinel-2 sensors. *Remote Sensing*, *14*(1), 229.

Singh, A., Jakubowski, A. R., Chidister, I., & Townsend, P. A. (2013). A MODIS approach to predicting stream water quality in Wisconsin. *Remote sensing of Environment*, *128*, 74-86.

Song, K., Li, L., Tedesco, L., Li, S., Duan, H., Liu, D., Hall, B., Du, J., Li, Z., & Shi, K. (2013). Remote estimation of chlorophyll-a in turbid inland waters: Three-band model versus GA-PLS model. *Remote sensing of Environment*, *136*, 342-357.

Sun, Y., Gao, P., Tariq, S., Azhar, A., ul Haq, Z., & Mehmood, U. (2023). Assessment of long-term trends in chlorophyll-a and sea surface temperature in the Arabian Sea and their association with aerosols using remote sensing. *Ocean & Coastal Management*, *242*, 106716.

Tesfaye, A. (2023). Water security problems of lake tana and its possible management options: A review. *East African Journal of Environment and Natural Resources*, *6*(1), 473-490.

Tibebe, D., Kassa, Y., Melaku, A., & Lakew, S. (2019). Investigation of spatio-temporal variations of selected water quality parameters and trophic status of Lake Tana for sustainable management, Ethiopia. *Microchemical Journal*, *148*, 374-384.

Tottrup, C., Druce, D., Meyer, R. P., Christensen, M., Riffler, M., Dulleck, B., Rastner, P., Jupova, K., Sokoup, T., & Haag, A. (2022). Surface water dynamics from space: a round robin intercomparison of using optical and SAR high-resolution satellite observations for regional surface water detection. *Remote Sensing*, *14*(10), 2410.

Tyler, A. N., Hunter, P. D., Spyrakos, E., Groom, S., Constantinescu, A. M., & Kitchen, J. (2016). Developments in Earth observation for the assessment and monitoring of inland, transitional, coastal and shelf-sea waters. *Science of the Total Environment*, *572*, 1307-1321.

Wale, A., Rientjes, T., Gieske, A., & Getachew, H. (2009). Ungauged catchment contributions to Lake Tana's water balance. *Hydrological processes: An international journal*, *23*(26), 3682-3693.

Wang, D., Tang, B.-H., Fu, Z., Huang, L., Li, M., Chen, G., & Pan, X. (2022). Estimation of Chlorophyll-A Concentration with Remotely Sensed Data for the Nine Plateau Lakes in Yunnan Province. *Remote Sensing*, *14*(19), 4950.

Wang, D., Tang, B.-H., & Li, Z.-L. (2024). Evaluation of five atmospheric correction algorithms for multispectral remote sensing data over plateau lake. *Ecological Informatics*, *82*, 102666.

Wang, J.-J., & Lu, X. (2010). Estimation of suspended sediment concentrations using Terra MODIS: An example from the Lower Yangtze River, China. *Science of the Total Environment*, *408*(5), 1131-1138.

Wang, N., Wang, Z., Huang, P., Zhai, Y., Yang, X., & Su, J. (2024). Inversion method for chlorophyll-A concentration in high-salinity water based on hyperspectral remote sensing data. *Sensors*, *24*(13), 4181.

Wang, X., Zhang, F., & Johnson, V. C. (2018). New methods for improving the remote sensing estimation of soil organic matter content (SOMC) in the Ebinur Lake Wetland National Nature Reserve (ELWNNR) in northwest China. *Remote sensing of Environment*, *218*, 104-118.

Womber, Z. R., Zimale, F. A., Kebedew, M. G., Asers, B. W., DeLuca, N. M., Guzman, C. D., Tilahun, S. A., & Zaitchik, B. F. (2021). Estimation of suspended sediment concentration from remote sensing and in situ measurement over Lake Tana, Ethiopia. *Advances in Civil Engineering*, *2021*(1), 9948780.

Wondie, A. (2012). Biodiversity and ecosystem services of lake Tana Wetlands, Ethiopia. *Biodiversity Conservation and Ecosystem Services for Climate Change Mitigation and Sustainable Development*, *20*, 91.

Wondie, A. (2018). Ecological conditions and ecosystem services of wetlands in the Lake Tana Area, Ethiopia. *Ecohydrology & Hydrobiology*, *18*(2), 231-244.

Wondie, A., Mengistu, S., Vijverberg, J., & Dejen, E. (2007). Seasonal variation in primary production of a large high altitude tropical lake (Lake Tana, Ethiopia): effects of nutrient availability and water transparency. *Aquatic Ecology*, *41*, 195-207.

Wondie, T. A. (2009). *The impact of urban storm water runoff and domestic waste effluent on water quality of Lake Tana and local groundwater near the city of Bahir Dar, Ethiopia* Cornell University Ithaca, NY, USA].

Worqlul, A. W., Ayana, E. K., Dile, Y. T., Moges, M. A., Dersseh, M. G., Tegegne, G., & Kibret, S. (2020). Spatiotemporal dynamics and environmental controlling factors of the Lake Tana water hyacinth in Ethiopia. *Remote Sensing*, *12*(17), 2706.

Xia, K., Wu, T., Li, X., Wang, S., Tang, H., Zu, Y., & Yang, Y. (2024). A novel method for assessing water quality status using MODIS images: A case study of large lakes and reservoirs in China. *Journal of hydrology*, *638*, 131545.

Yang, H., Kong, J., Hu, H., Du, Y., Gao, M., & Chen, F. (2022). A review of remote sensing for water quality retrieval: progress and challenges. *Remote Sensing*, *14*(8), 1770.

Yang, Z., Reiter, M., & Munyei, N. (2017). Estimation of chlorophyll-a concentrations in diverse water bodies using ratio-based NIR/Red indices. *Remote Sensing Applications: Society and Environment*, *6*, 52-58.

Ye, H., Yang, C., Dong, Y., Tang, S., & Chen, C. (2024). A daily reconstructed chlorophyll-a dataset in South China Sea from MODIS using OI-SwinUnet. *Earth System Science Data Discussions*, *2024*, 1-35.

Zhang, C., Zhu, Z., Špoljar, M., Kuczyńska-Kippen, N., Dražina, T., Cvetnić, M., & Mleczek, M. (2022). Ecosystem models indicate zooplankton biomass response to nutrient input and climate warming is related to lake size. *Ecological modelling*, *464*, 109837.

Zhang, S., Wang, L., Wang, Y., Zhang, X., Zhu, Y., & Ma, G. (2024). Monitoring of low Chl-a concentration in Hulun Lake based on fusion of remote sensing satellite and ground observation data. *Remote Sensing*, *16*(10), 1811.

Zhang, Y., Ma, R., Duan, H., Loiselle, S., Zhang, M., & Xu, J. (2016). A novel MODIS algorithm to estimate chlorophyll a concentration in eutrophic turbid lakes. *Ecological Indicators*, *69*, 138-151.

Zheng, Y., Wang, J., Kondratenko, Y., & Wu, J. (2024). Research progress in surface water quality monitoring based on remote sensing technology. *International Journal of Remote Sensing*, *45*(7), 2337-2373.

Zhou, T., Li, Y., Jiang, B., Alatalo, J. M., Li, C., & Ni, C. (2023). Tracking spatio-temporal dynamics of harmful algal blooms using long-term MODIS observations of Chaohu Lake in China from 2000 to 2021. *Ecological Indicators*, *146*, 109842.

Zhu, Y., Li, Y., Bi, S., Lyu, H., Cai, X., Wang, H., Li, J., Li, J., & Xu, J. (2023). Spatial and temporal distribution analysis of dominant algae in Lake Taihu based on ocean and land color instrument data. *Ecological Indicators*, *155*, 110959.